

Raman Cooling of Atoms in Two and Three Dimensions

Nir Davidson, Heun-Jin Lee, Mark Kasevich, and Steven Chu

Physics Department, Stanford University, Stanford, California 94305-4060

(Received 24 August 1993)

Sodium atoms have been cooled in two and three dimensions with stimulated Raman transitions. Atoms in 2D have been cooled to $v_{\text{rms}} = 1.2\hbar k/M$, corresponding to an effective temperature of $T_{\text{eff}} = 1.7 \mu\text{K}$ while atoms in 3D have been cooled to $v_{\text{rms}} = 2.3\hbar k/M$, or $T_{\text{eff}} = 4.3 \mu\text{K}$.

PACS numbers: 32.80.Pj

Methods for laser cooling of atoms continue to improve rapidly. Atoms have been laser cooled by polarization gradient molasses in three dimensions to temperatures as low as $\sim 20T_{\text{rec}}$, where $T_{\text{rec}} = (\hbar k)^2/2Mk_B$ is defined as the photon recoil temperature [1]. There have been several proposals [2] and two experiments [3,4] to cool atoms along one dimension to effective temperatures below the photon recoil temperature. We report here the first results of the extension of our Raman cooling method [4] to two and three dimensions. We have cooled sodium atoms to an effective temperature [5] of $1.7 \mu\text{K}$, or $\sim 1.5T_{\text{rec}}$ in two dimensions and to $4.3 \mu\text{K}$, or $\sim 3.5T_{\text{rec}}$ in three dimensions. The cooling represents a velocity phase space compression of ~ 18 and ~ 15 times over polarization gradient cooling for two and three dimensions, respectively.

The basic idea of cooling with stimulated Raman transitions has been previously described in our demonstration of 1D cooling [4]. Consider an atom with two ground states $|1\rangle$ and $|2\rangle$ separated by a hyperfine splitting $\hbar\omega_{\text{HFS}}$ and an excited state $|3\rangle$. If the atom initially in state $|1\rangle$ is irradiated with pulses of light from two counterpropagating laser beams at frequencies ω_1 and ω_2 (and wave numbers $k = |\mathbf{k}_1| \approx |\mathbf{k}_2|$), where $\omega_1 - \omega_2 \sim \omega_{\text{HFS}}$, the two-photon Raman transition from $|1\rangle \rightarrow |2\rangle$ has twice the Doppler sensitivity of a single-photon transition. If the Raman frequency difference is tuned to the red of the two-photon resonance, an atom moving with velocity $+v$ (towards the ω_1 beam) will Doppler shift the transition into resonance. During the transition $|1\rangle \rightarrow |2\rangle$, the atom receives a momentum kick $2\hbar k$ towards $v=0$. By varying the difference frequency, atoms with any positive velocity can be pushed towards $v=0$. If the directions of the two Raman beams are reversed, an atom moving with velocity $-v$ can be made to receive a momentum kick towards $v=0$.

An optical pumping pulse tuned to the $|2\rangle \rightarrow |3\rangle$ transition is used to return the atoms back to state $|1\rangle$ after each Raman pulse. During the optical pumping process, the spontaneous emission back into the $|1\rangle$ state has a chance of leaving the atom near the $v=0$ state. The stimulated Raman excitation/optical pumping cycle is repeated, each time pushing more atoms towards the $v=0$ state.

If the process is to be effective, atoms must be loaded

into the trapped velocity state more efficiently than they are ejected from it. In practice this means that atoms near $v=0$ must be able to survive the application of many pulses before being excited out of the velocity trapped state. Thus, both the line shape and linewidth of the Raman transitions are tailored to minimize unwanted excitations. We use Blackman pulses [4] to reduce the off-resonant excitation due to the frequency sidelobes of the Raman pulses. Also, the duration of the Raman pulses is lengthened as the frequency difference of the Raman beams is swept towards resonance with the $v=0$ atoms so that they have increased velocity selectivity.

Raman cooling can be extended to two or three dimensions by adding Raman pulses originating from the other directions, as shown in Fig. 1(a). Unfortunately, this sequential approach would involve switching the direction of eight or twelve laser beams, and would be cumbersome to implement experimentally. Instead, we investigated configurations where all the Raman beams are pulsed on simultaneously. Possible simultaneous beam configurations are depicted for the 2D and 3D case in Figs. 1(b) and 1(c), respectively. The Raman frequency difference $\omega_1 - \omega_2$ is tuned to the red of the two-photon resonance, as in the 1D case.

The 2D configuration includes four Raman beam pairs;

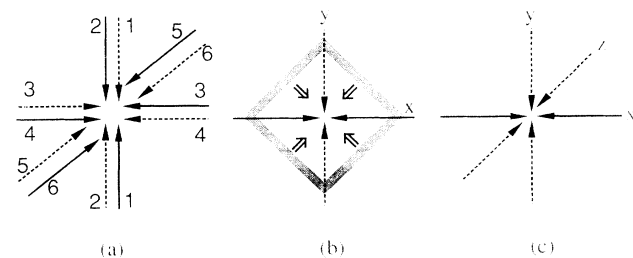


FIG. 1. The dashed lines denote ω_2 laser beams, and the solid lines denote ω_1 laser beams with $\omega_1 > \omega_2$. (a) Beam pairs labeled 1-6 are pulsed on sequentially to create a three dimensional velocity trapped state. (b) All four beams are pulsed simultaneously to create a two dimensional velocity trapped state. The four shaded areas illustrate the velocity classes that are excited for a certain red detuning of the Raman frequency difference. The double arrow denotes the direction of the $\sqrt{2}\hbar k$ momentum recoil kick of each velocity class. (c) The three dimensional generalization of (b).

each pair consists of one beam with frequency ω_1 , and one with frequency ω_2 . Each beam pair stimulates a Raman transition $|1\rangle \rightarrow |2\rangle$ if $\omega_1 - \omega_2 + \Delta\omega_{\text{Dopp}} - \Delta\omega_{\text{rec}} = \omega_{\text{HFS}}$, where the Doppler shift is $\Delta\omega_{\text{Dopp}} = (\mathbf{k}_1 - \mathbf{k}_2) \cdot \mathbf{v}$, and the recoil shift is $\Delta\omega_{\text{rec}} = \hbar k^2/M$. Thus, at a certain Raman frequency difference, a well defined velocity class is Doppler shifted into resonance for each of the four beam pairs, as shown in Fig. 1(b). Also shown in the figure is the direction of the momentum kick for each velocity class which has a component towards $v=0$. The magnitude of the momentum kick is $\sqrt{2}\hbar k$. As the Raman frequency difference is scanned, all atoms in the 2D velocity space may be addressed. The 3D configuration of Fig. 1(c) involves eight Raman beam pairs that act on the atoms in the 3D velocity space in a similar manner.

When an atom is irradiated with several Raman beams simultaneously, it can couple to a large number of momentum states during each Raman pulse by various multiphoton processes [6]. To account for such processes we numerically solved the Schrödinger equation for a three level atom in the beam configuration of Fig. 1(b). We used momentum eigenstates decomposition, and assumed that the detuning from the excited level $|3\rangle$ is large enough, so its population can be adiabatically eliminated [7]. Terms leading to standing wave diffraction (e.g., momentum changing terms involving absorption and emission from beams of the same frequency, but different directions) have been suppressed. Experimentally, this can be achieved with $\sigma^+\sigma^-$ polarizations for counterpropagating beams. Figure 2 shows the excitation probability $p(\mathbf{v})$ and the average velocity kick per pulse $\langle \Delta\mathbf{v} \rangle$ (the average is performed over the final momentum states) vs velocity \mathbf{v} calculated for a typical set of parameters. Note that $\langle \Delta\mathbf{v} \rangle$ tends to push atoms into the

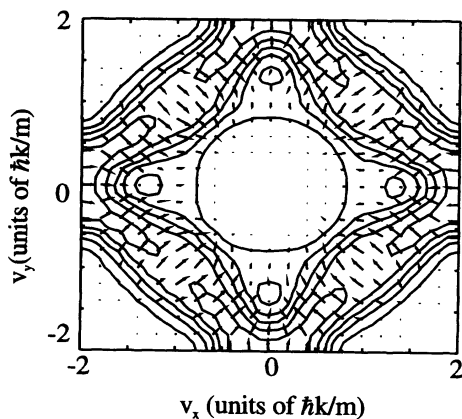


FIG. 2. Contour plot of the excitation probability $p(\mathbf{v})$ vs \mathbf{v} in the configuration shown in Fig. 1(b), for $\omega_1 - \omega_2 = 2\Delta\omega_{\text{rec}} + \omega_{\text{HFS}}$, and a Blackman π pulse with effective Rabi frequency of $\Delta\omega_{\text{rec}}$. Contour levels are incremented from 0 at (0,0) and $(\pm 2, \pm 2)$ by 0.16. Arrows indicate direction and strength of the average velocity kick $\langle \Delta\mathbf{v} \rangle$. The maximum average velocity kick is $1.8\hbar k/M$.

trapped velocity state, in general agreement with the intuitive picture of Fig. 1(b).

To demonstrate the multidimensional Raman cooling we started in a similar way to that of the previous 1D Raman cooling experiment. A beam of thermal Na atoms was slowed by a counterpropagating, frequency chirped laser beam [8], and loaded into a magneto-optic trap (MOT) [9]. A cw dye laser supplied the slowing and the trapping beams. Approximately 10^7 atoms were loaded in 160 msec. Then, the trapping magnet was shut off, and the trapping light intensity decreased for 20 msec, to further cool the atoms to a temperature of $\sim 35 \mu\text{K}$ (and $\sim 3 \text{ mm}$ FWHM diameter). Finally, the atoms were optically pumped into the $3S_{1/2}, F=1$ ground state.

For the 2D Raman cooling experiment we used the beam configuration of Fig. 1(b). A beam from a second cw dye laser, tuned $\sim 30 \text{ GHz}$ below the $3S_{1/2}, F=2$ to $3P_{3/2}, F=3$ transition was divided into two $\sim 250 \text{ mW}$ beams by a 30 MHz acousto-optic modulator (AOM). The undeflected beam passed through an electro-optic phase modulator with $\omega_{\text{RF}} \approx 1.7 \text{ GHz}$, to generate the Raman frequency difference [10]. The two beams were made to nearly copropagate through an additional AOM that provided the Blackman pulse shaping. The beams were then collimated to $\sim 5 \text{ mm}$ $1/e^2$ diameter, directed in perpendicular paths to the MOT, and retroreflected to provide the two other beams of Fig. 1(b). The polarizations of each counterpropagating Raman beam pair were $\sigma^+\sigma^-$, and the magnetic field was kept below 5 mG to suppress shifts of the Zeeman sublevels. Each cooling cycle lasted 150 μsec , and consisted of six Blackman shaped Raman pulses with total durations of 8, 18, 20, 20, 30, and 40 μsec and a Raman frequency difference detuned 600, 500, 400, 280, 180, and 100 kHz, respectively, from the two-photon resonance for $v=0$ atoms. An $\sim 1 \mu\text{sec}$ optical pumping pulse (tuned midway between the $3S_{1/2}, F=2$ to $3P_{3/2}, F=1$ and $3S_{1/2}, F=2$ to $3P_{3/2}, F=2$ transitions) was applied after each Raman pulse. The direction of the optical pumping beam was normal to the cooling plane, and was reversed after each cooling cycle with a Pockels cell and a polarizer. The intensity of the optical pumping pulse that yielded the best cooling was $\sim 100 \text{ mW/cm}^2$.

The velocity distribution of the Raman cooled atoms was measured with another velocity selective Raman transition between the $3S_{1/2}, F=1$ and $3S_{1/2}, F=2$ states. The number of atoms making the transition to the $F=2$ state was determined by measuring the fluorescence from a short pulse of light resonant with the $3S_{1/2}, F=1$ to $3P_{3/2}, F=3$ transition. The velocity resolution of this detection scheme was $\sim 0.1\hbar k/M$. By using different configurations of the Raman detection beams, we measured the velocity distribution along several directions. The results of such a measurement for the (1,1) direction of Fig. 1(b) after $\sim 5 \text{ msec}$ of Raman cooling are shown in Fig. 3, together with the initial velocity distribution (after cooling in optical molasses). As seen, the velocity

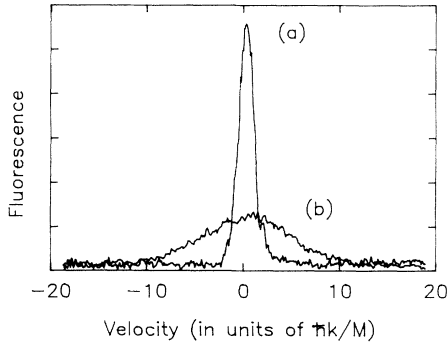


FIG. 3. The velocity distribution of sodium atoms along the (1,1) direction of Fig. 1(b) (a) after 5 msec of 2D Raman cooling, and (b) due to polarization-gradient cooling.

spread of the atoms along this axis decreased from $v_{(1,1),\text{rms}} = 4\hbar k/M$ to $v_{(1,1),\text{rms}} = 0.75\hbar k/M$. The velocity spreads along the directions of the Raman beams [(1,0) and (0,1) directions of Fig. 1(b)] were wider by $\sim 40\%$ than that of the (1,1) and (1, -1) directions. This is consistent with a velocity distribution with square (rather than circular) velocity contours [11], where the sides of the squares are perpendicular to the directions of the recoil kicks, depicted in Fig. 1(b). The velocity spread for such a 2D square velocity distribution can be shown to be $v_{\text{rms}} = 1.6v_{(1,1),\text{rms}} = 1.2\hbar k/M$, corresponding to an effective temperature of $1.7\ \mu\text{K}$, or $\sim 1.5T_r$. The number of atoms near $v_{(1,1)} = 0$ increased by a factor of 4.8, corresponding to a factor of ~ 18 increase in the number of atoms near $v_x = v_y = 0$. The total number of atoms (the area under the velocity distribution curve) remained constant to within $\sim 10\%$. The $1/e$ equilibrium time for loading the atoms into the trapped state was 1.8 msec.

We studied several loss mechanisms for atoms near the $v=0$ state. First, since the cooling was performed in a vertical plane, the atoms were accelerated downward by gravity at a rate of one recoil velocity every 3 msec. This results in a loss of $\sim 2.5\%$ from the $v \approx 0$ state for a 150 μsec cooling sequence and $v_{\text{rms}} \approx \hbar k/M$.

Second, atoms may be excited from the trapped velocity state by multiphoton processes. Two-photon standing wave processes are suppressed for the $\sigma^+\sigma^-$ polarization that we used. However, higher order processes (such as $\omega_1\omega_2\omega_2\omega_1$ transitions) cannot be totally suppressed in our beam arrangement. Numerical solutions of the Schrödinger equation for a three level atom, similar to those of Fig. 2, indicate that the excitation probability of the atoms near $v=0$ is $p(v=0) \approx 0.1\%$ for each of our 150 μsec pulse sequences. However, this value is extremely sensitive to the effective Rabi frequency of the Raman transitions Ω_{eff} , and increases to $p(v=0) \approx 20\%$ when Ω_{eff} is doubled (from 25 to 50 kHz). Since the variations of the ac stark shifts among the magnetic sublevels may be of the order of Ω_{eff} , and are not included in our simulations, $p(v=0)$ as high as 20% may not be excluded.

Atoms near the $v=0$ state might also undergo off-resonant excitation by either the Raman beams (that are ~ 30 GHz away from resonance) or the optical pumping beams (that are ~ 1.7 GHz away from resonance for the $3S_{1/2}, F=1$ state). By measuring the shift of the velocity distribution of the atoms at $3S_{1/2}, F=1$ state after applying several hundred optical pumping pulses from one direction, we found that atoms in that state scatter on average $\sim 8 \times 10^{-4}$ photons per optical pumping pulse, or $\sim 0.5\%$ for each cooling cycle. The off-resonant excitation by the Raman beams was evaluated by applying an identical Raman pulse sequence as in the cooling experiment on atoms initially in the $3S_{1/2}, F=1$ state, but with the 1.7 GHz sideband turned off, and measuring the fraction of the atoms that have undergone spontaneous Raman transition into the $3S_{1/2}, F=2$ state. After correcting for the atoms that were excited by the Raman beams and decayed back into the $3S_{1/2}, F=1$ state, the total off-resonant excitation probability for each cooling cycle was found to be 6%.

A final loss mechanism might occur when spontaneously emitted photons excite atoms near the $v=0$ state. Since in our experiment the optical thickness of the atoms was only a few percent, this loss mechanism may be neglected. We verified this by decreasing the number of atoms in the MOT by a factor of ~ 5 , and observing no improvement in the cooling temperature.

The measurements and calculations described above indicate that for our experiments the major loss mechanisms from the $v \approx 0$ state are gravity, off-resonance excitation by the Raman beams, and possibly multiphoton processes. Since our computer simulations ignore all the Zeeman sublevel structure we cannot compare the observed temperature of the Raman cooled atoms to the calculations. In particular, the multiphoton processes need to be understood better. The higher temperatures obtained in 2D Raman cooling (compared to the 1D case [4]) are caused by slower loading into the $v=0$ state and higher loss rates from it. The slower loading is due to the term $(\delta v/v_{\text{rec}})^n$ in the loading rate [4] (δv is the width of the dark state, and n is the dimension), and the higher loss rates are due to gravity, multiphoton processes, and off-resonance excitation by the additional Raman beams present in the 2D case.

For Raman cooling in a dipole trap [12] the loss mechanisms from the $v \approx 0$ state can be largely reduced. If a linearly polarized dipole trapping light is tuned far from resonance relative to the ground state hyperfine splitting, the ac Stark shift of any ground state level (regardless of F and m_F) will be nearly the same; hence, the Raman transitions between any two ground state levels will remain in resonance as the atoms move about in the trap. The atoms will be supported against gravity and the longer cooling time will enable us to decrease the intensities of the Raman beams (to suppress multiphoton processes), and to increase their detuning from the optical transition (to decrease off-resonance excitations). Final-

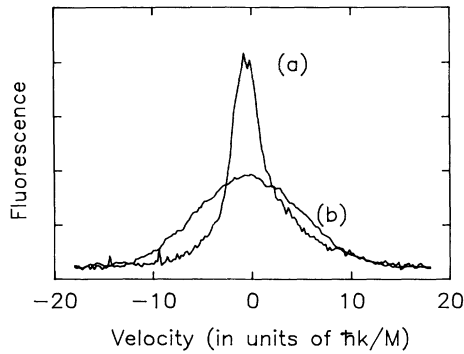


FIG. 4. The velocity distribution of sodium atoms along the (1,1,0) direction of Fig. 1(c) (a) after 5 msec of 3D Raman cooling, and (b) due to polarization-gradient cooling.

ly, the combination of dipole trapping and Raman cooling should be able to produce high densities of ultracold atoms.

We also performed initial experiments in 3D Raman cooling. The beam configuration was composed of three retroreflected beam pairs in the X , Y , and Z directions, similar to that of Fig. 1(c). The X and Y beams were identical to those of the 2D case. However, the frequency of the Z beams (ω_Z) was upshifted from that of the Y beams ($\omega_2 = \omega_0 - 30$ MHz) by 60 MHz using an additional AOM (i.e., $\omega_Z = \omega_0 + 30$ MHz), thereby eliminating standing wave diffraction due to YZ beam pairs. At the same time the XZ beam pairs contain a Raman frequency difference identical to that of the XY pairs $\omega_Z - (\omega_0 - \omega_{RF}) = (\omega_0 + \omega_{RF}) - \omega_2 = \omega_1 - \omega_2$, thus we have Raman cooling in both the XY and the XZ planes, as in the simpler configuration of Fig. 1(c) [13]. Finally, standing wave diffraction from antiparallel beam pairs was suppressed by using $\sigma^+ \sigma^-$ polarizations, as in the 2D case. All the beam intensities, detunings, and pulse sequences were identical to the 2D case. Figure 4 depicts the velocity distribution of the atoms along the (1,1,0) direction of Fig. 1(c) before and after ~ 5 msec of 3D cooling. The velocity spread of the atoms along this direction decreased from $4\hbar k/M$ to $1.45\hbar k/M$. The velocity spread along other directions was between 0% and 15% smaller, so the 3D velocity spread was $v_{rms} \approx (0.925)\sqrt{3}v_{(1,1,0),rms} = 2.3\hbar k/M$. The corresponding 3D effective temperature of the cooled atoms was $4.3 \mu\text{K}$, or $\sim 3.5T_{rec}$. The 3D velocity phase space compression was ~ 15 times.

This work was done with support from AFOSR and the NSF. N. Davidson was a Rothschild fellow during the course of this work.

-
- [1] See articles contained in the special issue on laser cooling and trapping of atoms [J. Op. Soc. Am. B 6 (1989)].
 - [2] D. E. Pritchard, K. Helmerson, V. S. Bagnato, G. P. Lalyatis, and A. G. Martin, in *Laser Spectroscopy VIII*, edited by W. Persson and S. Svanberg (Springer-Verlag, Berlin, 1987); H. Wallis and W. Ertmer, J. Opt. Soc. Am. B 6, 2211 (1989); K. Molmer, Phys. Rev. Lett. 66, 2301 (1991).
 - [3] A. Aspect, E. Arimondo, R. Kaiser, N. Vansteenkiste, and C. Cohen-Tannoudji, Phys. Rev. Lett. 61, 826 (1988); J. Opt. Soc. Am. B 6, 2112 (1989).
 - [4] M. Kasevich and S. Chu, Phys. Rev. Lett. 69, 1741 (1992).
 - [5] The effective temperature T_{eff} for an n dimensional velocity distribution is defined as $k_B T_{eff} = M V_{rms}^2/n$, where v_{rms}^2 is $\langle v_x^2 + v_y^2 \rangle$ in 2D and $\langle v_x^2 + v_y^2 + v_z^2 \rangle$ in 3D. We use the terminology "effective temperature" since the cooling usually leads to nonequilibrium and nonisotropic velocity distributions of the atoms, as was also done in Refs. [3] and [4].
 - [6] E. Arimondo, A. Bambini, and S. Stenholm, Phys. Rev. A 24, 898 (1981).
 - [7] K. Moler, D. S. Weiss, M. Kasevich, and S. Chu, Phys. Rev. A 45, 342 (1992).
 - [8] W. Ertmer, R. Blatt, J. L. Hall, and M. Zhu, Phys. Rev. Lett. 54, 996 (1985).
 - [9] A. Raab, M. Prentiss, A. Cable, S. Chu, and D. E. Pritchard, Phys. Rev. Lett. 59, 2631 (1987).
 - [10] The phase modulated beam actually contains three frequency components: a carrier (ω_0), an upper sideband ($\omega_1 = \omega_0 + \omega_{RF}$), and a lower sideband ($\omega_0 - \omega_{RF}$). The Raman transition is induced by the deflected AOM beam ($\omega_2 = \omega_0 - 30$ MHz) and ω_1 , where $\omega_{RF} + 30$ MHz $\approx \omega_{HFS}$. The carrier and lower sideband of the undeflected beam are shifted 30 and 60 MHz, respectively, from the two-photon resonance and do not stimulate Raman transitions (the Doppler shifts for our velocity distribution are less than 2 MHz FWHM).
 - [11] Such a velocity distribution is expressed in polar coordinates (v, Θ) as $\exp[-v^2/v_0^2(\Theta)]$, with $v_0(\Theta) = v_0(\Theta = \pi/4)/\sin(\Theta - \pi/4)$ for $\pi/4 < |\theta - \pi/4| < 3\pi/4$, and $v_0(\Theta) = v_0(\Theta = \pi/4)/\cos(\Theta - \pi/4)$ elsewhere.
 - [12] S. Chu, J. E. Bjorkholm, A. Ashkin, and A. Cable, Phys. Rev. Lett. 54, 314 (1986); J. D. Miller, R. A. Cline, and D. Heinzen, Phys. Rev. A 47, R4567 (1993).
 - [13] As in the 2D case, all other frequency differences are shifted by 30 or 60 MHz from the two-photon resonance.

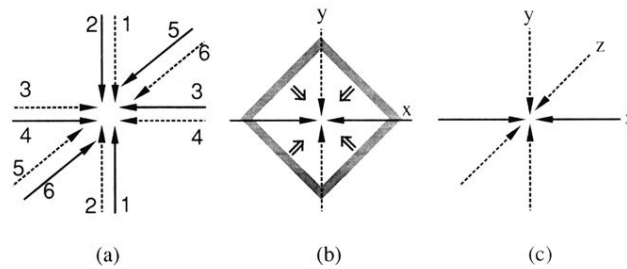


FIG. 1. The dashed lines denote ω_2 laser beams, and the solid lines denote ω_1 laser beams with $\omega_1 > \omega_2$. (a) Beam pairs labeled 1–6 are pulsed on sequentially to create a three dimensional velocity trapped state. (b) All four beams are pulsed simultaneously to create a two dimensional velocity trapped state. The four shaded areas illustrate the velocity classes that are excited for a certain red detuning of the Raman frequency difference. The double arrow denotes the direction of the $\sqrt{2}\hbar k$ momentum recoil kick of each velocity class. (c) The three dimensional generalization of (b).